https://dx.doi.org/10.4314/ijs.v26i1.4

PREPARATION OF STYRENE-BASED IMPRINTED POLYMER FOR THE ADSORPTION OF HAZARDOUS BROMOCRESOL GREEN DYE: EQUILIBRIUM, KINETICS AND THERMODYNAMICS STUDY

Awokoya, K. N.[1,*], Oninla, V. O.[1], Ogunkunle, O. A.[1], Oyebode, B. A.[2], Owoade, O. J.[3], Obitusin, O. O.[1] and Ipadeola, D.T.[1]

[1]Department of Chemistry, Obafemi Awolowo University, Ile-Ife, Nigeria.
[2]Department of Industrial Chemistry, First Technical University, Ibadan, Ibadan, Nigeria.
[3]Department of Chemistry, Lagos State University, P.O.Box 001, LASU Post Office, Lagos, Nigeria.
[*]Corresponding Author's Email: knawokoya@oauife.edu.ng; knawokoya@gmail.com
(Received: 1st February, 2024; Accepted: 20th March, 2024)

ABSTRACT

In this study, styrene was used as a functional monomer for the production of molecularly imprinted polymer (MIP) via free radical polymerization method, using bromocresol green dye (BCG) as template. A non-imprinted polymer (NIP), that excluded the template, was also synthesized. Both polymers were applied for the removal of BCG from aqueous medium. The synthesized polymers were characterized with Fourier transform infrared spectroscopy, scanning electron microscopy, and X-ray powder diffraction spectroscopic techniques. The effect of operating variables, such as pH, contact time, initial dye concentration and process temperature, on the efficiencies of the polymers in removing the dye were evaluated. Equilibrium time of BCG adsorption onto the MIP was reached within 40 min, with adsorption capacity of 49.68 mg g^{-1}. The adsorption process followed the pseudo-second-order kinetic and Freundlich isotherm models, while chemisorption mechanism was predicted. The adsorption process was spontaneous and exothermic in nature, with ΔH values of -140.03 and -25.01 kJ/mol^{-1} recorded for BCG removal by MIP and NIP, respectively. The styrene-based MIP showed good mechanical stability, and retained up to about 99% of its adsorption capacity after six sequential cycles of regeneration. Comparatively, the MIP (99.81mg g^{-1}) performed considerably better than its NIP (59.00 mg g^{-1}) analogue in the removal of BCG from aqueous medium, thus affirming the potentials of the molecular imprinting technique in the production of efficient adsorbents for adsorption of toxic dyes from industrial effluents.

Keywords: Bromocresol green, Adsorption, Imprinted polymer, Kinetic, Equilibrium.

INTRODUCTION

The huge production and massive utilization of synthetic dyes have resulted in substantial environmental pollution, thus, constituting a serious menace to the public. Dyes are primarily found in effluents released from rubber, plastics, dye processing, cosmetics, textile and leather industries (Nidheesh *et al.,* 2012; Linh *et al.,* 2019). The three primary groups of dyes are the anionic (which comprise acid, reactive, and direct dyes), cationic (which are majorly basic dyes), and the nonionic (*e.g.* disperse dyes). BCG (tetrabromocresolsulfonphthalein) is an anionic dye containing triarylmethane backbones. The dye has found use as a tracking agent for DNA agarose gel electrophoresis. Other areas of application include its use in protein determinations, as pH indicator, and in complexation processes involving charge-transfer (Ghaedi *et al.,* 2012). BCG is among a class of dyes commonly referred to as sulfonephthaleins, and is a member of the benzofurans. The free acid form of the dye is in form of light brown solid, while its sodium salt form is dark green solid. The dye is used in thin layer chromatography to visualize compounds whose functional groups has pK_a that is below 5.0. The complete biodegradation of BCG is very difficult and complex because of its multiplex aromatic molecular structures (Hassan and Carr 2018; Yavuz *et al.,* 2011). Many industrial dyes, BCG inclusive, are toxic even at low concentrations, causing many harmful effects on human beings, such as eye diseases and nausea upon ingestion. They disturb and affect the marine life, food cycle and have even showed evidences as potential candidates to cause cancer (Yuzhu and Viraraghavan 2002; Purkait and Dasgupta 2005; Faraji *et al.,* 2010). In order to avert potential ecological degradations and counter toxicological effects, a number of remediation methods have been developed for the removal of BCG from aqueous solutions. These comprise

reverse osmosis, precipitation, irradiation, ion exchange, oxidation, bio-sorption, photocatalysis, adsorption, flocculation, membrane filtration, coagulation, and integrated approaches (Banat *et al.,* 1996; Babu *et al.,* 2007; Zaharia *et al.,* 2007; Ali *et al.,* 2011). Unfortunately, many of the earlier mentioned methods are found to be capital intensive – they involve multiple operations and require high operational energy, thereby hampering their full-scale industrial applications (Nwabanne *et al.,* 2018).

Adsorption, on the other hand, is considered as a promising and affordable technique. Its advantages over other techniques include its ease of operation and high efficiency. Other advantages are: availability of a wide range of adsorbent materials, high possibility of regeneration and reuse, and low-energy requiring technology (Kanawade and Gaikwad, 2011; Priya *et al.,* 2014; Anjum *et al.,* 2017). Few of the adsorbent materials so far explored for adsorption purpose include sugarcane bagasse, chitin, maize cob, hazelnut shell, microorganisms such as fungus and yeasts, zeolites, lignin-based hydrogels and activated carbon (Jiang *et al.,* 2020; Li *et al.,* 2021; Wang *et al.,* 2021; Sterenzon *et al.,* 2022). However, as promising as these adsorbents are, many failed in their selectivity towards particular analytes, while others suffer from attrition, rendering them non-reusable (Awokoya *et al.,* 2019, 2021); hence the need for the development of alternative adsorbents that are capable of overcoming the deficiencies of common adsorbents.

Molecularly imprinted polymer (MIP) is a promising adsorbent because of its high specificity and selectivity towards analytes; its applicability in harsh chemical media; its high accessible specific cavities; its repeated use without loss of activity and its high mechanical strength (Awokoya *et al.,* 2013). Owing to these aforementioned reasons, MIPs have found usefulness in a wide area of applications (Muldoon *et al.,* 1997; Le Moullec *et al.,* 2006). They have been applied in membrane separation (Hosoya *et al.*, 1996), solid phase extraction (Zhu *et al.,* 2009), in vivo detection (Erturk-Bergdahl *et al.,* 2019), and electrochemical sensing (Mazzotta *et al.,* 2022). A typical MIP is prepared, simply by the copolymerization of a functional monomer with a crosslinker in the presence of a target analyte (template molecule), a porogenic solvent and an initiator. The template is subsequently removed, thus leaving binding cavities that are compatible with the shape, size, and functionality of the template within the polymeric network (Awokoya *et al.,* 2013; Mazzotta *et al.,* 2022).

The intention of this work was to introduce a styrene-based imprinted polymer as a high-quality adsorbent, followed by its utilization in the removal of BCG from aqueous solution. The specific objectives of the work included the characterization of the synthesized polymer, using SEM to investigate the morphology of the material; FTIR spectroscopy to identify functional groups; and XRD to identify the crystalline orientation of the polymer. The work also involved the fitting of experimental data into various isotherm and kinetic models such as the Langmuir, Freundlich, pseudo-first-order, pseudo-second-order and Elovich models. The thermodynamics of the process was also investigated.

MATERIALS AND METHODS

Bromocresol green, styrene, benzoyl peroxide (BPO) and divinyl benzene (DVB) were procured from Sigma-Aldrich (Germany). Other materials used include acetic acid, methanol and distilled water. All chemicals and reagents were used as obtained.

Instruments/Equipment

X-ray diffractometry analysis (for the determination of the crystallinity and phase of the polymers) was conducted by the use of a Bruker D8 Advance X-ray diffractometer with Cu Kα radiation (Germany). The surface structure and morphology of the materials were characterized using a Zeiss 6100 ultra plus FEGSEM (Germany). FTIR spectra were obtained on a Thermo Fisher Scientific Nicolet Avatar 330 spectrometer (USA) at a wavenumber range of 650 - 4000 cm^{-1}.

Procedure for the Preparation of Imprinted and Non-Imprinted Polymers

The synthesis was carried out according to the method of Awokoya *et al.,* 2021. A 422 mg sample

of BCG (template molecule), 200 mg of benzoyl peroxide (initiator) and 5 mL of distilled water were separately measured and mixed in a 100 mL standard flask for 10 min. Afterwards, 60 mL (524.2 mmol) of styrene (functional monomer) and 2.5 mL (17.3 mmol) of crosslinking agent were added to the flask. The mixture was stirred at 600 rpm for another 10 min at room temperature. The standard flask containing the mixed solutions was then placed on a heating module and heated at 70 °C for 30 min to obtain a very hard polymer. The resulting polymer was ground with pestle and mortar. Template removal was performed by 10 – times hourly repeated washing of the ground polymer with 300 mL of ratio 9:1 (v/v) mixture of methanol/acetic acid. The washing process was monitored using UV/Vis spectrophotometer. The resulting material was dried for 24 h and thenceforth referred to as molecularly imprinted polymer (MIP**)**. The non-imprinted polymer (NIP) variant was similarly synthesized, following the same procedure, but without the addition of template (BCG). This was to serve as a control. Scheme 1 shows the MIP preparation process**.**

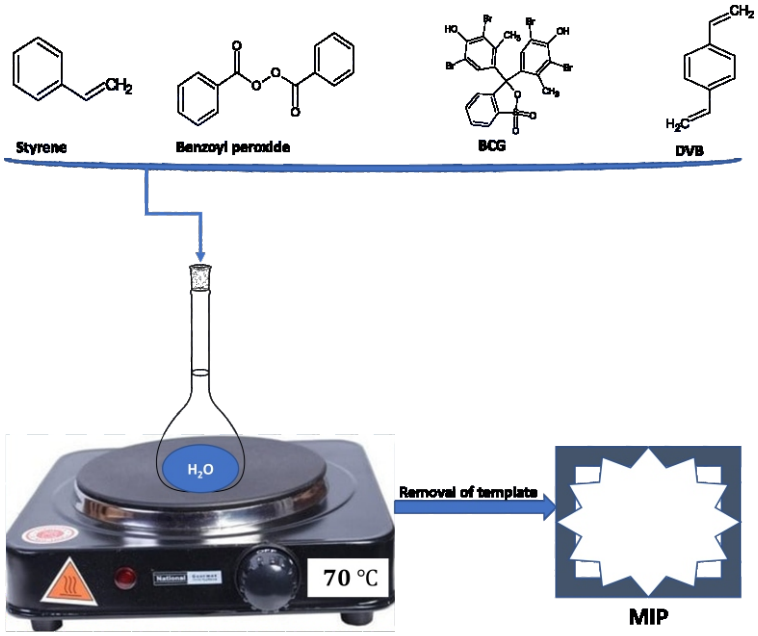

Scheme 1: Preparation process of the MIP

BCG Removal Experiment

BCG removal was performed in a batch adsorption procedure. The experiment was performed to investigate the effect of the pH of the dye solution, time of contact, temperature, and initial BCG concentration. To investigate the effect of pH, 50 mg polymer was separately added to a 20 mL solution of 100 mg L^{-1} BCG of varying pH, and then agitated at room temperature for 1 h on a GFL shaker (Burgwedel, Germany). The pH of each solution was varied to the desired pH value (from 1 – 9), by the addition of drops of either or both HCl and NaOH (0.1 – 1 M). The supernatant was separated by centrifugation (6000 rpm for 10 min), and the amount of dye removed was estimated by the use of a Shimadzu 1800 UV-vis spectrophotometer (Canby, Oregon, USA) to measure the remaining concentration in the supernatant at the wavelength of 442 nm. The studies on the effects of other parameters were similarly conducted as described for the effect of pH. With the exception of the parameter under study, all other parameters were kept constant at their optimum values, or properly defined. For the effect of time, agitation time was varied from 5 to 120 min; for temperature dependent study, temperature was varied from 30 to 60 °C; while the concentration of BCG was varied from 10 to 200 mg L^{-1} for concentration dependent study. The reusability of the MIP was investigated by repeating the adsorption-desorption experiments six (6) times. Desorption of the dye from the spent MIP was performed by using a mixture of MeOH and acetic acid (9:1). The quantity q_e (mg g^{-1}) and percentage BCG dye adsorbed (%) were estimated according to equations 1 and 2:

$$q_e = \frac{(C_o - C_e)V}{m} \quad 1$$

$$\% ads = \frac{C_o - C_e}{C_o} \times 100 \quad 2$$

Where C_o and C_e (mg L^{-1}) respectively stand for initial and equilibrium BCG concentrations; m (g) stands for mass of MIP or NIP; while V (L) represents volume.

Modelling of the Kinetics, Isothermal Behavior and the Thermodynamics of the Process

To probe the mechanism of BCG adsorption, experimental data were fitted into the equations of the following models: pseudo-first-order (Equation 3), pseudo-second-order (Equation 4), Elovich (Equation 5) and Weber and Morris (W-M) (for kinetic study) (Weber and Morris 1963; Lagergren 1898; Ho and McKay 1999); and two most broadly used adsorption isotherms: Langmuir (Equation 6) and Freundlich (Equation 7) (Freundlich 1906; Langmuir 1918; Singh and Mishra 2010). Investigation of the thermodynamics of the adsorption process, was undertaken by fitting adsorption data into the van't Hoff's equation (Equation 8). Linear plots of the models were obtained, and required parameters were quantified from the values of slopes and intercepts of the various plots. The Gibb's free energy (ΔG°) was calculated using Equation 9.

$$\ln(q_e - q_t) = \ln q_e - k_1 t \quad 3$$

$$\frac{t}{q_t} = \frac{t}{q_e} - \frac{1}{k_2 q_e^2} \quad 4$$

$$q_t = \frac{1}{\beta}\ln \alpha\beta + \frac{1}{\beta}\ln t \quad 5$$

$$\frac{C_e}{q_e} = \frac{C_e}{q_{max}} + \frac{1}{(K_a q_{max})} \quad 6$$

$$\log q_e = \log k_f + \frac{1}{n}\log C_e \quad 7$$

$$\ln K_c = \frac{\Delta S^{\circ}}{R} - \frac{\Delta H^{\circ}}{RT} \quad 8$$

$$\Delta G^{\circ} = \Delta H^{\circ} - T\Delta S^{\circ} \quad 9$$

Where qe and qt (mg g^{-1}) denote equilibrium BCG adsorbed; t (min) represents adsorption time; k_1 (min^{-1}) and k_2 (g/mg min) respectively represent pseudo-first-order and pseudo-second-order rate constants; α (mg/min) and β (g/mg) are constants; C_e (mg L^{-1}) denote the residual BCG concentration in solution at equilibrium; q_{max} (mg g^{-1}) stands for maximum adsorption capacity; K_a (L mg^{-1}) and k_f (mg g^{-1}) signify Langmuir and Freundlich constants, respectively; while n denote Freundlich intensity constant. The equilibrium constant, K_c, is defined as (C_a represents the concentration of the BCG on the polymer); the gas constant is represented by R (8.314 J $mol^{-1}K^{-1}$); whereas, T represents temperature in Kelvin (K).

RESULTS AND DISCUSSION

Characterization of MIP and NIP

The FTIR spectra, X-ray diffraction patterns and SEM images of all the adsorbents are depicted in Figure 1. For FTIR (Figure 1A), it was observed that the spectrum of the synthesized MIP showed vibrational peaks that are very similar to its non-imprinted counterpart. This similarity in the backbone structure confirmed that the BCG template molecule has been successfully removed from the synthesized *MIP*. All the spectra show a particular peak at 2918 cm^{-1}. This peak has been ascribed to $C-H$ stretching (da Silva *et al.,* 2020). The vibrational peak at 1490 cm^{-1} is ascribable to the $C-C$ vibrations of the polymeric network (Dinali *et al.,* 2021), while the peak at 1449 cm^{-1} confirms the existence of $C=C$ stretching vibrations in the aromatic rings from styrene, DVB and BPO (Gupta and Kumar, 2011). Of all the three spectra, only the spectrum of MIP_{after} (after adsorption) exhibited a distinct peak at 1181 cm^{-1}. This peak is characteristic of the $S=O$ of the SO_3 group of the BCG dye. Thus, confirming the adsorption of BCG molecule in the MIP_{after} material. The XRD patterns of MIP_{after}, MIP_{before} and NIP are presented in Figure. 1B. All the three diffractograms showed the same features. No apparent changes in the crystal ordered arrangement were observed before and after adsorption. The two distinct crystalline peaks that were observed in all the diffractograms with the strongest peak around 20.92° and a shoulder peak in the region 13.98° correspond to the anhydrous crystal size of the polymers (Awokoya *et al.,* 2018). The morphologies of the MIP_{after} (after

absoption), MIP_{before} (before adsorption) and NIP were observed by SEM (Figure. 1C-E). The SEM micrograph of the MIP_{before} showed large lumps of aggregated particles with the formation of cavities of different sizes that revealed the porous nature of the surface of the material. After the adsorption of BCG (MIP_{after}), a change in surface morphology was observed: a reduction in the sizes of the aggregated particles was observed. This was, most possible, as a result of the interaction of the dye with the MIP. As can be seen in the NIP micrograph, the non-imprinted polymer had a more smooth, regular and uniform shape than its imprinted counterparts, probably, due to the absence of the template cavities. The more irregular and rougher surface observed in the MIP, when compared with the NIP, could be responsible for the much better BCG removal efficiency recorded, thus strongly suggesting that the formation of template cavities on the MIP played a significant role in its adsorption performance. This phenomenon has been observed in our previous studies where pyrrole and pyridine were used as the molecular templates, and styrene was used as functional monomer to prepare MIP by bulk polymerization (Awokoya *et al.,* 2021).

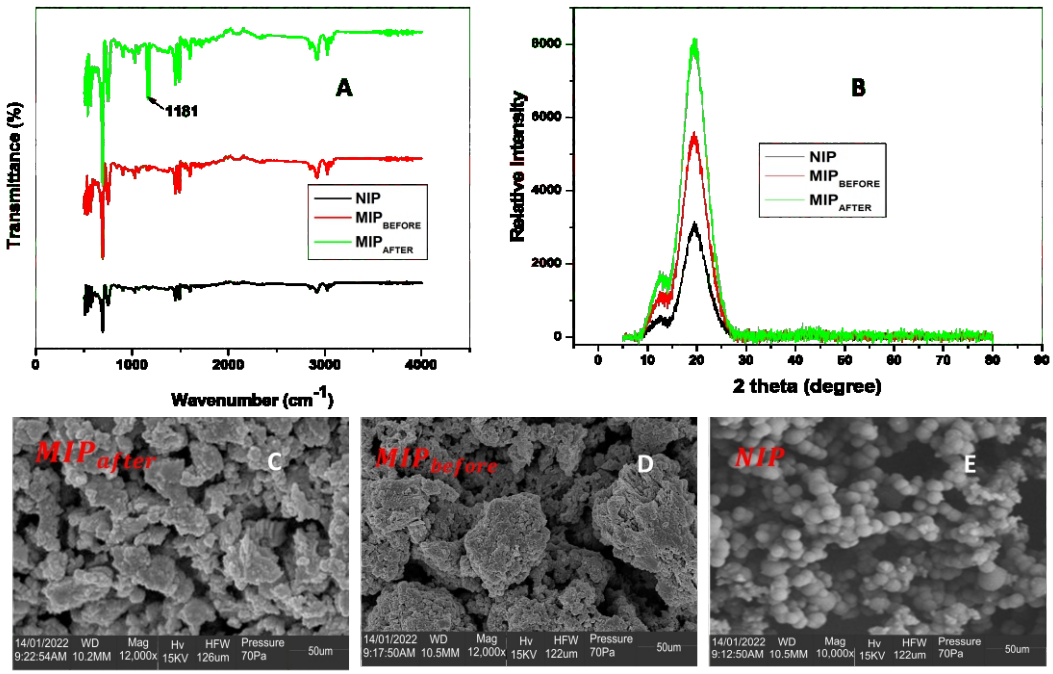

Figure 1 *FTIR spectra* (A), *X – ray diffraction patterns* (B) *and SEM images of the polymers* $(C - E)$

Adsorption of BCG

Effect of pH on the Adsorption of BCG

The pH of an adsorbate solution is considered to be a very crucial parameter influencing the adhesion of adsorbate molecules to the surface of adsorbents. Its influence involves alteration of adsorbent's surface charge and adsorbate form in solution (Zhao *et al.,* 2021). The effect of pH on the adsorption of BCG onto both the MIP and NIP was investigated under a batch adsorption study. The chosen experimental condition involved fixing adsorbent dose at 50 mg; agitation time at 60 min; BCG concentration at 100 mg L^{-1}; and temperature at 27 ± 1 °C. As presented in Figure 2a, a similar profile was obtained for the adsorption of BCG on both the MIP and NIP. With MIP as the adsorbent, a slight rise in BCG uptake, from 97.8 to 98.2%, was observed with increase in solution pH from 1 to 2. After the initial rise, a gradual decrease in BCG uptake was observed, reaching about 89.2% at pH = 9. Hence, optimum adsorption was observed at pH = 2. This possibly implies that at acidic pH = 2, the number of H^+ ion in the solution was very high, resulting in electrostatic attraction which favoured the adsorption of BCG onto the MIP surface (Liu *et al.,* 2019). Comparing the adsorption performance of the MIP and NIP at the optimum pH = 2, it was discovered that the adhesion of BCG on the MIP was over 2-fold the performance of NIP (98.2% by MIP and 46.8% by NIP). This, therefore, highlights the significance of molecular

imprinting technology in the preparation of efficient adsorbents. For subsequent studies, pH = 2 was maintained as the solution pH.

Effect of Agitation Time on the Adsorption of BCG

The resultant effect of varying the agitation time on BCG removal by both the MIP and NIP was studied. As shown in Figure 2b, early rapid increase in BCG adsorption was observed within the first 20 min for both the MIP and NIP adsorbents. The rate of the dye uptake became gradually slower after 20 min, and attained equilibrium after 40 min. At equilibrium, about 49.68 and 23.40 mg g^{-1} of BCG were removed by MIP and NIP, respectively. As observed under the pH dependent study, the performance of the MIP was over 2-fold that of the NIP at equilibrium. As depicted in the time dependent adsorption profile, the rapid dye adsorption observed at the early phase of the process could be attributed to the availability of large number of accessible binding sites, occasioned by the cavities created at the surface of the MIP. These binding sites later became substantially occupied over time, thereby resulting in electrostatic repulsions between the adsorbed and incoming BCG molecules. After 40 min, equilibrium adsorption/ desorption rate was observed (Bentahar *et al.,* 2018).

Effect of dye Concentration on the Adsorption of BCG

Highly coloured wastewaters from textiles and related factories often contain a diverse range of dyes in high concentrations (Tkaczyk *et al.,* 2020), hence the need to estimate the quantity of dye that a fixed amount of adsorbent can efficiently remove. The concentration effect on BCG removal is depicted in Figure. 2c. BCG concentration was varied from 10 to 200 mg L^{-1}, while all other parameters were kept constant. The obtained result showed that BCG uptake increased as the initial concentration of the dye became increased. When BCG concentration was 50 mg L^{-1}, the observed uptake by the MIP and NIP were 24.51 and 10.34 mg g^{-1}, respectively. Upon concentration increase to 200 mgL^{-1}, the quantity of BCG adsorbed were found to be 99.81 and 59.00 mg g^{-1} for MIP and NIP, respectively. At low dye concentration, few BCG molecules were available for binding. This resulted in near complete removal of the dye molecules in solution. However, as shown in the effect of concentration profile, the resultant quantity adsorbed was apparently small. With increasing dye concentration, more dye molecules became available for binding. This resulted in increasing amount of BCG adsorbed up to 200 mg L^{-1} (the highest BCG concentration investigated). The steady rise in dye uptake (up to 200 mg L^{-1}) implies that the number of cavities on the adsorbent can sufficiently accommodate the binding of BCG molecules at concentrations beyond 200 mg L^{-1} (Fernandes *et al.,* 2020).

Kinetics Modeling of BCG Adsorption

The kinetics as well as the mechanism of BCG adsorption onto the synthesized MIP and NIP were evaluated from the intercepts and slopes of the kinetic models' plots (linear) of the time dependents data. Values of the various kinetic parameters were recorded as precented in Table 1.

Table 1: Kinetic model (linearized equations) and the values of parameters estimated from their plots (PFO pseudo – first – order, PSO pseudo – second – order & Elovich).

Kinetic model	Linearized equation	Parameter	*MIP*	*NIP*
PFO	$\ln(q_e - q_t) = \ln q_e - k_1 t$	R^2	0.7720	0.2822
		$k_1\ (L\ min^{-1})$	0.0655	0.0344
		$q_{e(exp)}(mg\ g^{-1})$	7.9019	1.3509
		$q_{e(calc)}(mg\ g^{-1})$	15.887	7.1132
PSO	$\frac{t}{q_t} = \frac{t}{q_e} - \frac{1}{k_2 q_e^2}$	R^2	0.9998	0.9997
		$k_2\ (g\ mg^{-1} min^{-1})$	0.0153	0.0474
		$q_{e(exp)}(mg\ g^{-1})$	50.251	23.640
		$q_{e(calc)}(mg\ g^{-1})$	50.464	23.663
Elovich	$q_t = \frac{1}{\beta}\ln[\alpha\beta] + \frac{1}{\beta}\ln t$	R^2	0.9456	0.8133
		α	2.81E+12	1.67E+4
		β	0.2029	0.2985

As evaluated by the value of the determination coefficient, R^2, the best fit of the experimental data was ascribed to the pseudo-second-order model, with R^2 = 0.9998 for MIP and 0.9997 for NIP. This postulation was corroborated by the closeness of both the calculated and experimental q_e values obtained for the pseudo-second-order model ($q_{e(exp)}$ was estimated as was estimated as 50.25 mg g^{-1} (for MIP) and 23.64 mg g^{-1} (for NIP), while $q_{e(calc)}$ was estimated as 50.46 mg g^{-1} (for MIP) and 23.66 (for NIP)). On the other hand, a marked difference in the estimated q_e values were obtained for the pseudo-first-order model as revealed in table 1, thereby suggesting that the adsorption of BCG onto MIP/NIP failed to follow the pseudo-first-order kinetic model. The best fitting by the pseudo-second-order model implies that the adsorption process was mostly controlled by chemical interactions between BCG molecules and the surfaces of the polymers. The pseudo-second-order model assumes that the overall rate of adsorption is measured by the rate of diffusion of adsorbate in the available sites or cavities on the adsorbent material (Plazinski *et al.,* 2013). Elovich equation model has been broadly applied to chemisorption data and mostly useful in a heterogeneous adsorbing surface (Cheung *et al.,* 2000). The R^2 values of about 0.8133 to 0.9456 obtained for the Elovich model demonstrate substantial fits, thereby indicating the possible involvement of chemisorption, which mostly involves the formation of chemical bonds, triggered by electrons sharing between adsorbents and adsorbates (Sterenzon *et al.,* 2022). This finding is in concordance with the one previous reported for the removal of BCG by chitosan poly(methacrylate) composites (Liu *et al.,* 2019).

Isothermal Modeling of BCG Removal

To describe the dye distribution and the types of adsorbate layers formed during the adsorption process, studies based on various adsorption isotherm models are important. The isothermal behavior of BCG adsorption onto MIP/NIP was

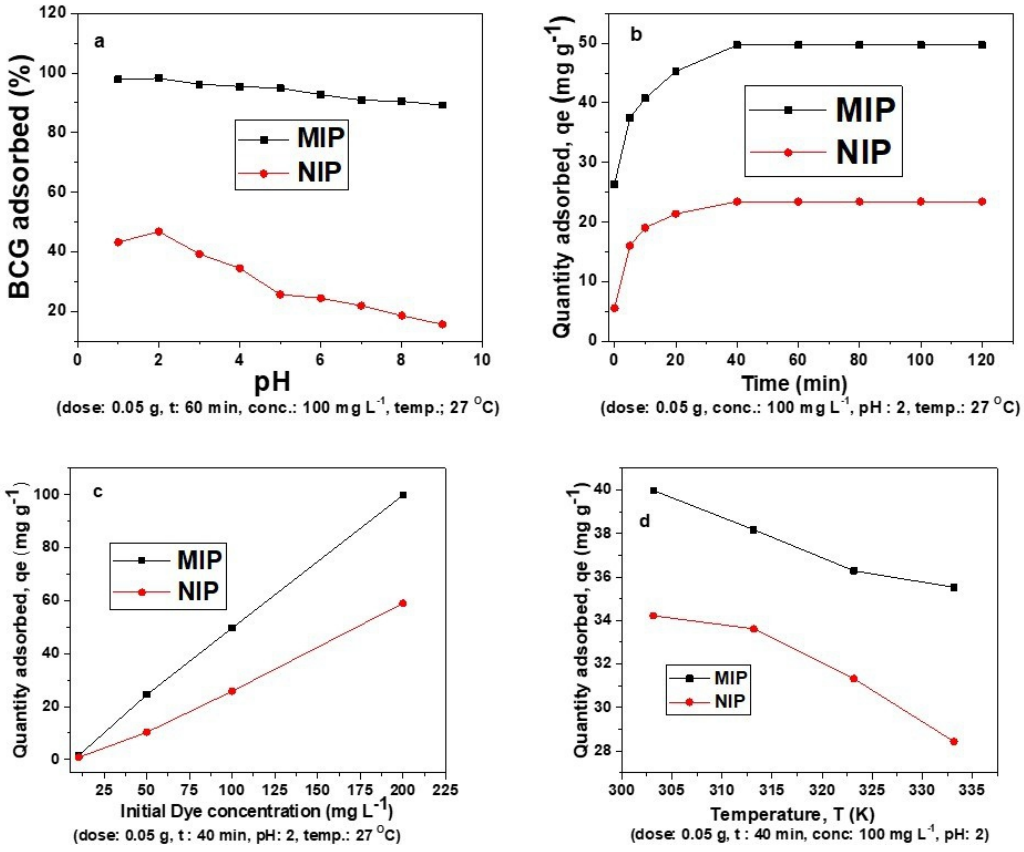

Figure 2 *Plots of the effects of (a) pH, (b) contact time, (c) initial concentration, and (d) temperature on the adsorption of BCG by* ***MIP/NIP***

explored using the two widely-known models: Freundlich and Langmuir models as shown in Table 2. The Langmuir isotherm is a semi-empirical relation that was originally formulated for gas-solid interactions, but now used for all manner of adsorbents (Elmorsi 2011). This model has been used in describing the following: monolayer adsorption, constant adsorption energy, homogeneous adsorption sites, and absence of cross interaction between the adsorbates. On the other hand, Freundlich isotherm has been applied in the description of multilayer adsorption on heterogeneous sites. Its postulates are based on the non-equivalence of the adsorption heat distribution and adsorbate attractions at the heterogeneous surface (Foo and Hammed, 2010). The Langmuir constants q_{max} and K_a values, as well as the Freundlich constants and and k_f were estimated from the intercepts and slopes of the linear plots of the experimental data, and shown in Table 2. Freundlich model had higher calculated values of R^2: R^2 = 0.9971 (MIP) and 0.9969 (NIP) compared to the Langmuir model: R^2 = 0.9948 (MIP) and 0.6473 (NIP); indicating that the surface of the MIP/NIP can be said to be heterogeneous as regards the removal of BCG. The values of lie between zero and one, an indication of favourable adsorption of BCG onto MIP/NIP.

Influence of Temperature and Thermodynamics of Adsorption of BCG

Temperature is a major parameter in adsorption reactions. The experimental results show that rise in temperature had unfavorable effect on BCG removal. The quantity of BCG adsorbed decreased with increase in the operational temperature. The decrease in the amount of BCG adsorbed on the MIP/NIP with rise in temperature could be due to the possible weakening of the π – π forces between the molecules of the dye and the MIP/NIP surfaces. A careful observation of the obtained profile, Figure 2d, shows that the highest quantity of the dye (39.98 mg g^{-1} for MIP and 34.22 mg g^{-1} for NIP) was removed at 30 °C, while the least

Table 2: Isothermal model (linearized equations) and the values of parameters estimated from their plots

Isothermal model	Linearized equation	Parameter	*MIP*	*NIP*
Langmuir	$\frac{1}{q_e} = \frac{1}{q_{max} K_{LC_e}} + \frac{1}{q_{max}}$	R^2	0.9948	0.6473
		$k_L\ (L\ mg^{-1})$	-0.0492	0.0124
		$q_{max}(mg\ g^{-1})$	46.73	9.35
Freundlich	$\ln q_e = \ln k_f + \frac{1}{n} \ln C_e$	R^2	0.9971	0.9969
		$k_F\ (L\ mg^{-1})$	7.00E-4	6.45E-5
		1/n	0.4195	0.9011

Table 3: Thermodynamic parameters obtained for the adsorption of BCG onto MIP and NIP.

Parameter	Temperature (K)	*MIP*	*NIP*
$\Delta H\ (kJmol^{-1})$		-140.03	-25.009
$\Delta S\ (kJmol^{-1}K^{-1})$		-0.4102	-0.0671
$\Delta G\ (kJmol^{-1})$	303	-15.739	-4.6777
	313	-11.637	-4.0067
	323	- 7.535	-3.3357
	333	- 3.433	-2.6647

Table 4: Adsorptive performance of the MIP in comparison with some selected adsorbent materials

Material	Dose (g)	*Conc* $(mg\ L^{-1})$	$q_{max}\ (mg\ g^{-1})$ *BCG*
This study	0.05	10 – 200	46.73
Chitosan poly(methacrylate)	0.01	05 – 100	39.84 (*Liu et al.*, 2019)
Ziziphus nummularia	0.80	10 – 200	19.61 (*Shokrollahi et al.*, 2011)
Acid functionalized rice husk	2.00	50 – 300	19.34 (*Onu et al.*, 2023)
Chitin nanofibres	1.50	0.2–2.00	18.02 (*Salmalian et al.*, 2019)

adsorption was observed at 60 °C with 35.53 mg g^{-1} for MIP and 28.44 mg g^{-1} for NIP. The parameters obtained from the thermodynamic treatment of the adsorption data are as presented in Table 3. The change in Gibbs free energy (ΔG^{o}) calculated was negative, for the sorption of BCG on MIP and NIP, at all the temperatures investigated. This suggests that the process was spontaneous and feasible (Oninla *et al.* 2022). The negative values obtained for the entropy change (ΔS^{o}) and enthalpy change (ΔH^{o}) imply a decrease in disorderliness at the solid/solution interface and the exothermic nature of the processes. The negative ΔH^{o} values also shows that the adsorption process was not favoured at higher temperatures, which is consistent with the effect of temperature results (Kumar *et al.,* 2014).

Regeneration and Reusability of the MIP

One crucial parameter for evaluating the economic usefulness of adsorbents is their regeneration and reusability. The likelihood of the regeneration as well as the reusability of the MIP was investigated by conducting a desorption study using a mixture of MeOH and acetic acid (9:1). As presented in Figure 3, the BCG removal percentage was 99.87% after the 1st cycle and this percentage apparently did not reduce up till the 6th regeneration-reusability cycles. The result indicates that the MIP had excellent stability and could be repeatedly used (at least up to six times) without deformation or activity loss.

Comparison of the activities of other Adsorbents with that of the MIP

The maximum BCG adsorption capacity of other adsorbents and that of the MIP used in this study have been compared and presented in Table 4. Overall, the MIP used in this study demonstrated superior adsorption capacity in comparison with some of the synthetic and natural adsorbents found in the literature.

CONCLUSION

In summary, the present study looked at how a styrene-based MIP could be employed for the sequestration of BCG from aqueous medium. The styrene-MIP was characterized using SEM, FT-IR and XRD. The BCG adsorption on MIP was substantially impacted by process parameters: pH, agitation time, initial dye concentration and temperature. At pH = 2 and room temperature, about 98.2% of the dye was removed. The MIP adsorbent exhibited excellent BCG removal due to its unique characteristics, such as abundance of cavities on its surface. BCG adsorption onto the MIP fitted well to the pseudo-second-order (kinetic) and Freundlich (isothermal) models, with the maximum monolayer adsorption estimated to be about 46.73 mg g^{-1}. Thermodynamic investigation depicted chemisorption as well as spontaneous and exothermic nature. It is noteworthy that the MIP showed high regeneration performance, with six sequential cycles of regeneration attained, without the loss of removal efficiency. thus making the adsorbent

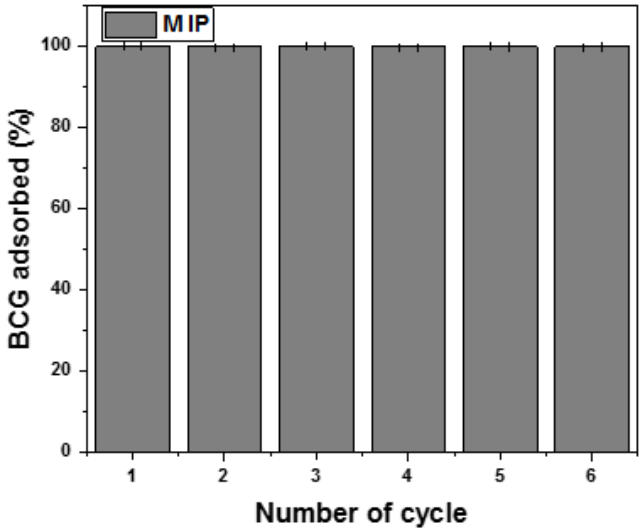

***Figure 3** Adsorption percentage of the **MIP for BCG** in six consecutive regenration cycles*

cost effective. The synthesized MIP exhibited a relatively high adsorption capacity, when compared with other values reported in the literature. Hence, it can be resolved that the MIP adsorbent appeared as a potential polymer material for the removal of BCG from aqueous medium.

ACKNOWLEDGEMENTS

The authors greatly appreciate the PSBC research group of the Department of Chemistry, Obafemi Awolowo University, Ile-Ife, Nigeria, for her support to carry out the experimental work in their Laboratory.

AUTHORS' CONTRIBUTIONS

All authors contributed to the conception and design of the study; data collection and analysis were performed by O.J.O., O.O.O., D.T.I. and B.A. O.; interpretation of results was performed by K.N.A., V.O.O. and O.A.O.; first draft of the manuscript was written by K.N.A.; final draft and English language editing was done by V.O.O. All authors reviewed and approved the final manuscript.

REFERENCES

Ali I, Khan TA, Hussain I (2011) Treatment and remediation methods for arsenic removal from the ground water. *International Journal of Environmental Engineering* 3: 48–71. doi:10.1504/IJEE.2011.037873.

Anjum NA, Gill SS, Tuteja N (2017) Enhancing Cleanup of Environmental Pollutants. Springer. Hardcover ISBN 978-3-319-55425-9; eBook ISBN 978-3-319-55426-6

Awokoya KN, Batlokwa BS, Moronkola BA, Chigome S, Ondigo DA, Tshentu Z, Torto N (2013) Development of a styrene based molecularly imprinted polymer and its molecular recognition properties of vanadyl tetraphenylporphyrin in organic media. *Inter J Polym Mat & Polym Biomater* 63: 107–113. doi:10.1080/00914037.2013.769255

Awokoya KN, Oninla VO, Adeleke IT, Babalola JO (2018) Preparation and characterization of methacrylic acid-based molecularly imprinted polymer as a new adsorbent for recognition of 1,4-dihydroxybenzene. *International Research Journal of Pure and Applied Chemistry* 16: 1-11. doi:10.9734/IRJPAC/2018/38586

Awokoya KN, Oninla VO, Babalola JO, Mbaeyi NN, Folorunso TJ, Ndukwe NA (2019) Adsorption of Malachite Green onto Styrene-Methacrylate Based Molecularly Imprinted Polymer. *Ife Journal of Science* 21: 67-80. doi:10.4314/ijs.v21i3.7

Awokoya KN, Okoya AA, Elujulo O (2021) Preparation, characterization and evaluation of a styrene-based molecularly imprinted polymer for capturing pyridine and pyrrole from crude oil. *Scientific African* 13: e00947. doi:10.1016/j.sciaf.2021.e00947

Babu BR, Parande AK, Raghu S, Kumar TP (2007). Textile technology. Cotton textile processing: Waste generation and effluent treatment. *Journal of Cotton Science* 11: 141–153.

Banat ME, Nigam P, Singh D, Marchant R (1996) Microbial decolourization of textile dye containing effluents, a review. *Biores Technol* 58: 217-227. doi:10.1016/s0960-8524(96)00113-7

Bentahar S, Dbik A, el Khomri M, el Messaoudi N, Lacherai A (2018) Removal of a cationic dye from aqueous solution by natural clay. *Groundwater for Sustain. Dev.* 6: 255–262. doi:10.1016/j.gsd.2018.02.002

da Silva DF, Ogawa CYL, Sato F, Neto AM, Larsen FH, Matumoto-Pintro PT (2020) Chemical and physical characterization of Konjac glucomannan-based powders by FTIR and ^{13}C MAS NMR. *Powder Technol* 361: 610-616. doi.org/10.1016/j.powtec.2019.11.071

Cheung CW, Porter JF, McKay G (2000) Elovich equation and modified second-order equation for sorption of cadmium ions onto bone char. J Chem Technol Biotechnol 75:963–970. doi: 10. 1002/ 1097- 4660(200011) 75:

Dinali LAF, de Oliveira HL, Teixeira LS, de Souza Borges W, Borges KB (2021) Mesoporous molecularly imprinted polymer core@shell hybrid silica nanoparticles as adsorbent in microextraction by packed sorbent for multiresidue determination of pesticides in apple juice. *Food Chem* 345: 128745.
doi: 10.1016/j.foodchem.2020.128745

Elmorsi TM (2011) Equilibrium Isotherms and Kinetic Studies of Removal of Methylene Blue Dye by Adsorption onto Miswak Leaves as a Natural Adsorbent. *J Environ Prot 2*: 817– 827.
doi: 10.4236/jep.2011.26093

Erturk Bergdahl G, Andersson T, Allhorn M, Yngman S, Timm R, Lood R (2019) *In vivo* detection and absolute quantification of a secreted bacterial factor from skin using molecularly imprinted polymers in a surface plasmon resonance biosensor for improved diagnostic abilities. *ACS Sens* 4: 717–725.
doi: 10.1021/acssensors.8b01642

Faraji M, Yamini Y, Tahmasebi E, Saleh A, Nourmohammadian F (2010) Cetyltrimethylammonium bromide-coated magnetite nanoparticles as highly efficient adsorbent for rapid removal for reactive dyes from the textile companies' wastewaters. *J Iran Chem Soc* 7:130–144.
doi: 10.1007/BF03246192

Fernandes JV, Rodrigues AM, Menezes RR, Neves GA (2020) Adsorption of anionic dye on the acid-functionalized bentonite. *Materials* 13: 3600.
doi: 10.3390/ma13163600

Foo KY, Hameed BH (2010) Insights into the Modeling of Adsorption Isotherm Systems. *Chem Eng J* 156: 2– 10.
doi: 10.1016/j.cej.2009.09.013

Freundlich HMF (1906) Uber die adsorption in lasungen, *Z. Phys Chem* 57, 385–470.

Ghaedi M, Khajesharifi H, Hemmati Yadkuri A, Roosta M, Sahraei R, Daneshfar A (2012) Cadmium hydroxide nanowire loaded on activated carbon as efficient adsorbent for removal of Bromocresol Green. *Spectrochim Acta Part* A 86: 62−68.
doi: 10.1016/j.saa.2011.09.064

Gupta R, Kumar A (2011) Synthesis and characterization of sol-gel-derived molecular imprinted polymeric materials for cholesterol recognition. *J Sol-Gel Sci Technol* 58: 182-194.
doi: 10.1007/s10971-010-2376-5

Hassan MM, Carr CM (2018) A critical review on recent advancements of the removal of reactive dyes from dyehouse effluent by ion-exchange adsorbents. *Chemosphere* 209: 201−219.
doi: 10.1016/j.chemosphere.2018.06.043.

Ho YS, McKay G (1999) Pseudo-second order model for sorption processes. *Process Biochem* 34: 451–465.
doi.org/10.1016/S0032-9592(98)00112-5

Hosoya K, Yoshizako K, Shirasu Y, Kimata K, Araki T, Tanaka N, Haginaka J (1996) Molecularly imprinted uniform-size polymer-based stationary phase for high-performance liquid chromatography structural contribution of cross-linked polymer network on specific molecular recognition. *J Chromatogr A* 728: 139–147.
doi: 10.1016/0021-9673(95)01165-X

Jiang C, Wang X, Hou B, Hao C, Li X, Wu J (2020) Construction of a Lignosulfonate−Lysine Hydrogel for the Adsorption of Heavy Metal Ions. *J Agric Food Chem* 68: 3050−3060.
doi: 10.1021/acs.jafc.9b07540.

Kanawade SM, Gaikwad RW (2011) Removal of Methylene Blue from Effluent by Using Activated Carbon and Water Hyacinth as Adsorbent. *International Journal of Chemical Engineering and Applications* 2: 317-319.
doi: 10.7763/IJCEA.2011.V2.126.

Kumar PS, Fernando PSA, Ahmed RT, Srinath R, Priyadharshini M, Vignesh AM, Thanjiappan A (2014) Effect of temperature on the adsorption of methylene blue dye onto sulfuric acid–treated orange peel. *Chem Eng Comm* 201:1526–1547.
doi: 10.1080/00986445.2013.819352

Lagergren S. (1898) About the theory of so-called adsorption of soluble substances, Kungliga Svenska Vetenskapsakademiens Handlingar Band 124: 1–39.

Langmuir I (1918) The adsorption of gases on plane surfaces of glass mica and platinum. *J Am Chem Soc* 40: 1361–1402. do: 10.1021/ja02242a004

Le Moullec S, Begos A, Pichon V, Bellier B (2006) Selective extraction of organophosphorus nerve agent degradation products by molecularly imprinted solid-phase extraction. *J Chromatogr* A 1108:7–13 doi:10.1016/j.chroma.2005.12.105.

Li X, Wang X, Han T, Hao C, Han S, Fan X (2021) Synthesis of Sodium Lignosulfonate-Guar Gum Composite Hydrogel for the Removal of Cu^{2+} and Co^{2}. *Int J Biol Macromol* 175: 459−472. doi: 10.1016/j.ijbiomac.2021.02.018.

Linh HX, Thu NT, Toan TQ, Huong DT, Giang BT, Ha HKP, Nguyen HTT, Chung NTK, Nguyen TK, Hai NT (2019) Fast and Effective Route for Removing Methylene Blue from Aqueous Solution by Using Red Mud-Activated Graphite Composites. *Journal of Chemistry* 1–7. doi:10.1155/2019/2858170.

Liu D, Li JYJ, Zhang G (2019) Preparation of Chitosan Poly(methacrylate) Composites for Adsorption of Bromocresol Green. *ACS Omega* 4: 12680−12686. doi: 10.1021/acsomega.9b01576.

Mazzotta E, Di Giulio T, Malitesta C (2022) Electrochemical sensing of macromolecules based on molecularly imprinted polymers: challenges, successful strategies, and opportunities. *Anal Bioanal Chem* doi.org/10.1007/s00216-022-03981-0

Muldoon MT, Stanker LH (1997) Molecularly Imprinted Solid Phase Extraction of Atrazine from Beef Liver Extracts. Analytical Chemistry 69: 803-808. doi:10.1021/ac9604649.

Nidheesh PV, Gandhimathi R, Ramesh ST (2013) Degradation of dyes from aqueous solution by Fenton processes: a review. Environmental Science and Pollution Research 20: 2099–2132. doi:10.1007/s11356-012-1385-z.

Nwabanne JT, Okpe EC, Asadu CC, Onu CE (2018) Sorption studies of dyestuffs on low-cost adsorbent. *Asian Journal of Physical and Chemical Sciences* 5: 1–19. doi: 10.9734/AJOPACS/2018/39338.

Oninla VO, Awokoya KN, Babalola JO, Balogun KI, Ismail OS (2022) Optimization of synthesis conditions for graft copolymerization of methacrylic acid onto *Garcinia kola* pods and use in the sequestration of cationic dyes from simulated wastewaters. doi:10.1007/s13399-022-03443-8.

Onu CE, Ekwueme BN, Ohale PE, Onu CP, Asadu CO, Obi CC, Dibia KT, Onu OO (2022) Decolourization of bromocresol green dye solution by acid functionalized rice husk: Artificial intelligence modeling, GA optimization, and adsorption studies. *Journal of Hazardous Materials Advances* 100224. doi: 10.1016/j.hazadv.2022.100224

Plazinski W, Dziuba J, Rudzinski W (2013) Modeling of sorption kinetics: the pseudo-second order equation and the sorbate intraparticle diffusivity. *Adsorption* 19:1055–1064. doi: 10.1007/s10450-013-9529-0

Priya R, Nithya R, Anuradha R, Kamachi T (2014) Removal of colour from crystal violet dye using low-cost adsorbents. *International Journal of ChemTech Research* 6: 4346-4351.

Purkait MK, DasGupta S, De S (2005) Adsorption of eosin dye on activated carbon and its surfactant- based desorption. *J Environ Manage* 76: 135–142. doi: 10.1016/j.jenvman.2005.01.012

Salmalian E, Rezaei H, Shahbazi A (2019) Removal of bromocresol green from aqueous solutions using chitin nanofibers. *Environ Resour Res* 7: 79-86. doi: 10.22069/IJERR.2019.4816

Shokrollahi A, Alizadeh A, Malekhosseini Z, Ranjbar M (2011) Removal of Bromocresol Green from Aqueous Solution via Adsorption on *Ziziphus nummularia* as a New, Natural, and Low-Cost Adsorbent: Kinetic and Thermodynamic Study of Removal Process. *Journal of Chem & Eng Data* 56: 3738-3746.
doi: 10.1021/je200311y

Singh DK, Mishra S (2010) Synthesis and characterization of Hg (II)-ion-imprinted polymer: Kinetic and isotherm studies. Desalination 257: 177–183.
doi: 10.1016/j.desal.2010.02.026

Sterenzon E, Vadivel VK, Gerchman Y, Luxbacher T, Narayanan R, Mamane H (2022) Effective Removal of Acid Dye in Synthetic and Silk Dyeing Effluent: Isotherm and Kinetic Studies ACS Omega 7: 118−128.
doi: 10.1021/acsomega.1c04111.

Tkaczyk A, Mitrowska K, Posyniak A (2020) Synthetic organic dyes as contaminants of the aquatic environment and their implications for ecosystems: a review. Sci Total Environ 717:137222.
doi: 10. 1016/j. scito tenv. 2020. 137222

Wang X, Li X, Peng L, Han S, Hao C, Jiang C, Wang H, Fan X (2021) Effective Removal of Heavy Metals from Water Using Porous Lignin-Based Adsorbents. Chemosphere 279: 130504.
doi: 10.1016/j.chemosphere.2021. 130504.

Weber WJ, Morris JS (1963) Kinetics of adsorption on carbon from solutions. J Sanit Eng Div Am Soc Civ Eng 89: 31–59.
doi:10.1061/jsedai.0000430.

Yavuz E, Bayramoğlu G, Arica MY, Senkal BF (2011) Preparation of poly (acrylic acid) containing core-shell type resin for removal of basic dyes. J Chem Technol Biotechnol 86: 699−705.
do: 10.1002/jctb.2571.

Yuzhu F, Viraraghavan T (2002) Removal of congo red from an aqueous solution by fungus aspergillus niger. Adv Environ Res 7: 239–247.
doi: 10.1016/S1093-0191(01)00123-X.

Zaharia C, Diaconescu, R, Surpăţeanu M (2007) Study of flocculation with Ponilit GT-2anionic polyelectrolyte applied into a chemical wastewater treatment. Central European Journal of Chemistry 5: 239-256.
doi:10.2478/s11532-006-0057-6.

Zhao GD, Zhao HJ, Shi L, Cheng BW, Xu XL, Zhuang XP (2021) A highly efficient adsorbent constructed by the *in-situ* assembly of zeolitic imidazole framework-67on 3D aramid nanofiber aerogel scaffold. Separation and Purification Technology 274: 119054.
doi: 10.1016/j.seppur.2021.119054.

Zhu Q, Wang L, Wu S, Joseph W, Gu X, Tang J (2009) Selectivity of Molecularly Imprinted Solid Phase Extraction for Sterol Compounds. Food Chemistry 113: 608–615.
doi: 10.1 016/j.foodchem.2008.07.044